# Yb-Diffused $LiNbO_3$ Annealed/Proton-Exchanged Waveguide Lasers

Masatoshi Fujimura, *Member, IEEE*, Hidekazu Tsuchimoto, and Toshiaki Suhara, *Senior Member, IEEE*

***Abstract*—Yb-diffused $LiNbO_3$ annealed/proton-exchanged waveguide lasers are demonstrated for the first time. Thermal diffusion of Yb into $LiNbO_3$ crystal is studied, and concentration profile of Yb is measured. A Fabry–Pérot waveguide laser of 3-cm length is fabricated and characterized. For optical pumping at 918-nm wavelength, stable continuous-wave laser oscillation is achieved at 1061 nm with a threshold power of 40 mW.**

***Index Terms*—Lasers, lithium niobate, optical waveguides, rare earth, ytterbium.**

## I. Introduction

RARE-EARTH-DOPED $LiNbO_3$ is an attractive material for waveguide devices because it can provide laser functions as well as electrooptic, acoustooptic, and nonlinear-optic effects. A variety of advanced waveguide laser devices have been demonstrated in Nd-doped [1]–[3] and Er-doped [4], [5] $LiNbO_3$. Yb-doped $LiNbO_3$ is also an attractive material. Yb in $LiNbO_3$ has only one excited manifold, and provides laser emission at $\sim$1.0-$\mu$m wavelength for optical pumping at $\sim$0.9 $\mu$m [6], [7]. Since there is no decrease of the excited-state population due to excited state absorption, efficient laser oscillation is expected in Yb : $LiNbO_3$. High performance of Yb as a light absorber in a Yb–Er codoped system is also expected [8], [9].

The first Yb : $LiNbO_3$ waveguide laser was demonstrated in a $Y$-propagation Ti-diffused waveguide [6]. Photorefractive damage in the waveguide prevented stable laser oscillation. Laser oscillation was also obtained in a $Z$-propagation Ti-diffused waveguide [7]. $Z$-propagation waveguide suffer less photorefractive damages. However, it does not provide access to the largest electrooptic/nonlinear-optic tensor components $r_{33}/d_{33}$ to limit future application.

In this letter, we demonstrate Yb-thermally diffused $Z$-cut $LiNbO_3$ annealed/proton-exchanged (APE) waveguide lasers. We chose APE waveguide for its high resistance to the photorefractive damage and possible access to $r_{33}/d_{33}$. Stable continuous-wave (CW) laser oscillation was achieved in a prototype device.

Manuscript received July 28, 2004; revised August 27, 2004. This work was supported by the Grants-In-Aid for Scientific Research form Ministry of Education, Culture, Sports, Science and Technology (MEXT), Japan.

The authors are with the Department of Electronic Engineering, Graduate Schools of Engineering, Osaka University, Osaka 565-0871, Japan (e-mail: fujimura@ele.eng.osaka-u.ac.jp; htsuchimoto@ele.eng.osaka-u.ac.jp; suhara@ele.eng.osaka-u.ac.jp).

Digital Object Identifier 10.1109/LPT.2004.837910

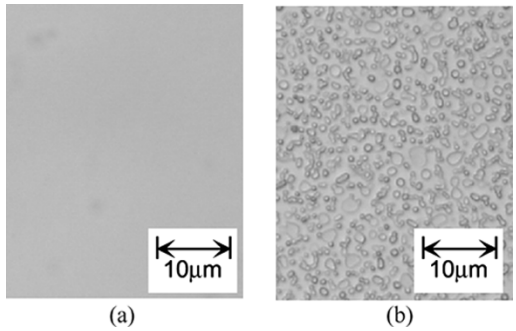


Fig. 1. Microscope photographs (x500) of $LiNbO_3$ crystal surfaces after diffusion of Yb films of (a) 48- and (b) 76-nm thicknesses.

## II. Yb-Diffusion Into Lithium Niobate Crystal

Although Yb-diffusion into $LiNbO_3$ has been reported [6], [7], it has not been examined in detail yet. We studied Yb-diffusion in preliminary experiments.

Yb films of various thicknesses were deposited on $-Z$ surfaces of $LiNbO_3$ by evaporation. The crystals were heated in oxygen atmosphere using a quartz tube furnace for Yb-diffusion. The diffusion temperature and the duration were determined to be 1100 °C and 250 h, respectively, after [6]. Smooth surfaces were obtained for diffusion of Yb films of $\leq$50-nm thicknesses, although diffusion of Yb films of $\geq$70 nm resulted in rough surfaces because of insufficient diffusion, as shown in Fig. 1. We fabricated Yb : $LiNbO_3$ by diffusion of Yb film of 30-nm thickness for further characterization and device fabrication.

Depth profile of Yb concentration was measured by spatially resolved fluorescence measurement [10]. The Yb-diffused surface was wedge-polished with an angle of 0.3° to the initial surface. Then the depth profile was converted and extended to the lateral profile along the slope of the wedge. A pump beam of 918-nm wavelength was loosely focused on the polished surface and the focal spot was scanned along the slope, as shown in the inset of Fig. 2. The spot size was $\sim$6 $\mu$m and the focal depth was $\sim$40 $\mu$m. Fluorescence of $\sim$1-$\mu$m wavelength from Yb was separated from the pump by a dichroic filter and detected. Circles in Fig. 2 show the detected fluorescence power $P_f$ dependent on the lateral shift of the focal spot $l$ [mm] and the corresponding depth, $d = l\tan(0.3°) \times 1000$ [$\mu$m]. As shown in Fig. 2 by a solid line, the data points were fitted very well by a complementary error function: $P_f(d) = k\mathrm{erfc}(d/6.5)$, where $k$ is a constant. Since $P_f$ is approximately proportional to the total number of Yb ions in the pumped region, derivative of $P_f(d)$ gives depth profile of Yb concentration: $C(d) = C_0 \exp\{-(d/6.5)^2\}$. The result shows that the depth profile can

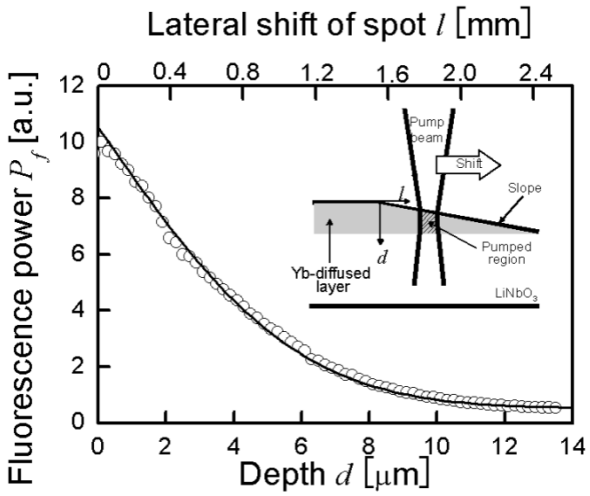


Fig. 2. Fluorescence power dependent on lateral shift of spot position and the corresponding depth. Inset shows the experimental setup.

be approximated by a Gaussian function with surface concentration of $C_0$ and 1/e-depth of 6.5 $\mu$m. The diffusion coefficient was found to be 0.04 $\mu m^2/h$ for 1100 °C. $C_0$ can be correlated to the thickness of the diffusion source assuming that all Yb ions in the source diffuse into the crystal. Then $C_0$ is estimated to be $1.3 \times 10^{20}$ ions/cm$^3$.

## III. Characterization of Waveguides

An Al film with channel openings was fabricated on a Yb-diffused $LiNbO_3$ as a mask for selective proton exchange. The length of the channel was 30 mm, and the width ranged from 4 to 10 $\mu$m. The crystal was soaked in molten benzoic acid at 200 °C for 20 min for proton exchange, and thermally annealed at 370 °C for 60 min in oxygen atmosphere. A transverse-magnetic (TM)-polarized wave of 918-nm wavelength was coupled in the waveguides by end-fire coupling. The full-width at half-maximum mode sizes were 3.1 $\mu$m in width and 2.3 $\mu$m in depth for waveguides of 4-$\mu$m width. The waveguide loss was measured by the Fabry–Pérot method [11] to be $0.5 \pm 0.2$ dB/cm at 1064-nm wavelength, where optical absorption due to Yb is not remarkable.

A white light from a halogen lamp was coupled in the waveguide, and the spectrum of the transmitted light was measured. Comparing the spectrum with that for nondoped $LiNbO_3$ APE waveguide, the absorption spectrum of the Yb in the waveguide was obtained, as shown in Fig. 3. Three absorption peaks were found at 918, 980, and 1008 nm. The absorption at 918 nm was measured to be 77%. From the absorption, Yb concentration profile, and the guided mode profile, we estimated the absorption cross section to be $5.2 \times 10^{-21}$ cm$^2$. It agrees fairly well to the previously reported value for $LiNbO_3$ crystal Yb-doped during crystal growth [9]. Fluorescence spectrum was measured for optical pumping at 918 nm. Fluorescence peaks were obtained at 980, 1008, and 1061 nm, as shown in Fig. 4. The decay time of the fluorescence power for pumping by a chopped beam was measured, and the result indicated that the lifetime of the excited state was about 290 $\mu$s. It is smaller than the reported value for Ti : Yb : $LiNbO_3$ waveguides [6], [7]. The reduction

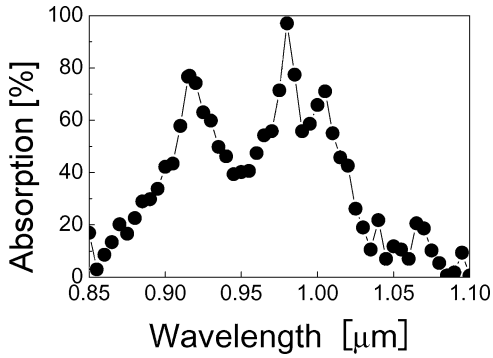


Fig. 3. Absorption spectrum of a Yb : $LiNbO_3$ APE waveguide of 30-mm length.

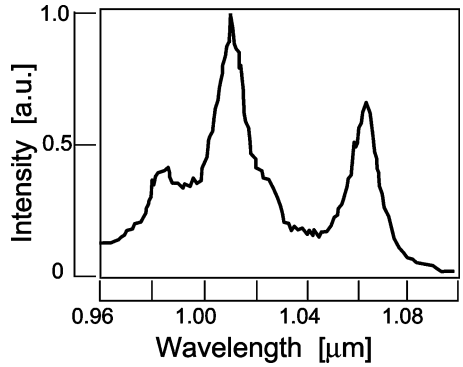


Fig. 4. Fluorescence spectrum of a Yb : $LiNbO_3$ APE waveguide optically pumped at 918-nm wavelength.

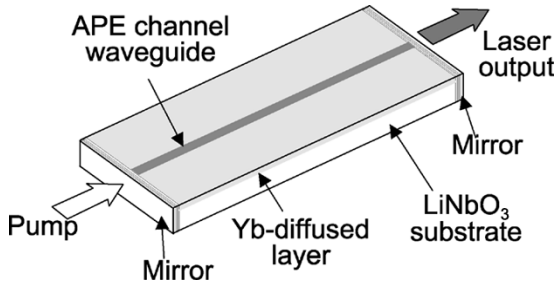


Fig. 5. Yb-diffused $LiNbO_3$ APE waveguide laser.

may be attributed to nonradiative transition caused by phonons due to OH band vibration in the APE waveguides [12].

## IV. Demonstration of Laser Oscillation

Fig. 5 shows schematic illustration of the fabricated waveguide laser. A Fabry–Pérot laser cavity was constructed by attaching identical mirrors on both facets of the waveguide using an ultraviolet adhesive. The mirror reflectivities were 4% at 918-nm wavelength and >99.9% at 1061 nm. An input wave of ~1064-nm wavelength was coupled in the cavity, and the transmitted power was recorded with scanning the input wavelength. The cavity finesse was estimated to be ~10, which agreed very well to the theoretical value estimated from the measured propagation loss and the mirror reflectivity.

A TM-polarized pump wave of 918 nm from a Ti : $Al_2O_3$ laser was coupled in the device from a facet. No photorefractive damage was observed, and stable CW laser oscillation was

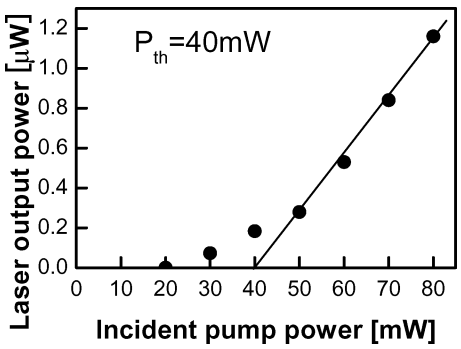


Fig. 6. Laser output power dependent on pump power.

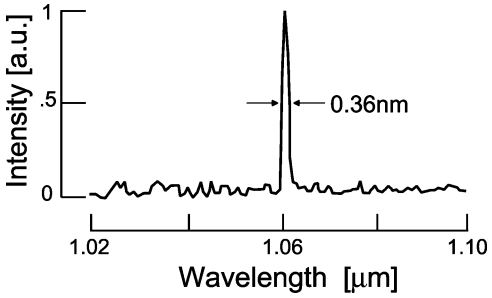


Fig. 7. Spectrum of the laser emission.

achieved at 1061 nm. Fig. 6 shows the output power of the oscillating laser light emitted from a facet dependent on the pump power for a device of 5-$\mu$m channel width. The pump power was measured in front of the pump facet. The oscillation threshold was 40 mW, and an output power up to 1.2 $\mu$W was obtained so far. The slope efficiency was $3 \times 10^{-5}$. A laser emission spectrum was measured and is shown in Fig. 7. The wavelength bandwidth was 0.36 nm. The spectrum probably consisted of about 40 longitudinal modes, although the individual modes were not observed because of the insufficient resolution in the measurement.

The measured oscillation threshold and slope efficiency were compared with theoretical values obtained by a calculation based on rate equation analysis [13]. In the calculation, the measured values for the mode size, the scattering loss, and the lifetime were used. For the cross sections of absorption and stimulated emission, the values reported in [9] were used. The theoretical oscillation threshold was 21 mW. The measured threshold was rather higher. The discrepancy is attributed mainly to the coupling loss of the pump wave into the waveguide cavity due to field mismatch between the incident pump beam and the guided mode. A slope efficiency for a mirror reflectivity of 99.99% at oscillation wavelength with an assumption of 50% input-coupling loss was calculated to be $4 \times 10^{-5}$, which is comparable to the measured value of $3 \times 10^{-5}$.

## V. Conclusion

Yb-diffused $LiNbO_3$ APE waveguide lasers were demonstrated for the first time. Future work includes improvement of laser performance by optimization of cavity design.

## References

[1] E. Lallier, D. Papillon, J. P. Pocholle, M. Papuchon, M. De Micheli, and D. B. Ostrowsky, "Short pulse, high power $Q$-switched Nd : MgO : $LiNbO_3$ waveguide laser," *Electron. Lett.*, vol. 29, pp. 175–176, Jan. 1993.

[2] J. Amin, M. Hempstead, J. E. Roman, and J. S. Wilkinson, "Tunable coupled-cavity waveguide laser at room temperature in Nd-diffused Ti : $LiNbO_3$," *Opt. Lett.*, vol. 19, pp. 1541–1543, Oct. 1994.

[3] M. Fujimura, T. Kodama, T. Suhara, and H. Nishihara, "Quasiphase-matched self-frequency-doubling waveguide laser in Nd : $LiNbO_3$," *IEEE Photon. Technol. Lett.*, vol. 12, pp. 1513–1515, Nov. 2000.

[4] C. Becker, T. Oesselke, J. Pandavenes, R. Ricken, K. Rochhausen, G. Schreiber, W. Sohler, H. Suche, R. Wessel, S. Balsamo, I. Montrosset, and D. Sciancalepore, "Advanced Ti : Er : $LiNbO_3$ waveguide lasers," *IEEE J. Sel. Topics Quantum Electron.*, vol. 6, pp. 101–113, Jan./Feb. 2000.

[5] G. Schreiber, D. Hofmann, W. Grundkotter, Y. L. Lee, H. Suche, V. Quiring, R. Ricken, and W. Sohler, "Nonlinear integrated optical frequency converters with periodically poled Ti : $LiNbO_3$ waveguides," in *Proc. SPIE*, vol. 4277, May 2001, pp. 144–160.

[6] J. K. Jones, J. P. de Sandro, M. Hempstead, D. P. Shepherd, A. C. Large, A. C. Tropper, and J. S. Wilkinson, "Channel waveguide laser at 1 $\mu$m in Yb-indiffused $LiNbO_3$," *Opt. Lett.*, vol. 20, pp. 1477–1479, 1995.

[7] J. Amin, J. A. Aust, D. L. Veasey, and N. A. Sanford, "Dual wavelength, 980 nm-pumped, Er/Yb-codoped waveguide laser in Ti : $LiNbO_3$," *Electron. Lett.*, vol. 34, pp. 456–458, Mar. 1998.

[8] E. Cantelar, R. Nevado, G. Martin, J. A. Sanz-Garcia, G. Lifante, F. Cusso, M. J. Hernandez, and P. L. Pernas, "Optical properties of Er and Yb co-doped lithium niobate waveguides," *J. Luminescence*, vol. 87–89, pp. 1096–1098, May 2000.

[9] C. Huang and L. McCaughan, "Polarization-dependent enhancement of population inversion and of green upconversion in Er : $LiNbO_3$ by Yb codoping," *IEEE Photon. Technol. Lett.*, vol. 5, pp. 599–601, May 1997.

[10] M. Hempstead, "Determination of diffusion profiles of neodymium in lithium niobate by means of spatially resolved fluorescence measurements," *J. Appl. Phys.*, vol. 74, pp. 5483–5492, Nov. 1993.

[11] R. Regener and W. Sohler, "Loss in low-finesse Ti : $LiNbO_3$ optical waveguide resonators," *Appl. Phys. B*, vol. 26, pp. 143–147, Mar. 1985.

[12] P. Baldi, M. P. De Micheli, K. El Hadi, S. Nouh, A. C. Cino, P. Aschieri, and D. B. Ostrowsky, "Proton exchanged waveguides in $LiNbO_3$ and $LiTaO_3$ for integrated lasers and nonlinear frequency converters," *Opt. Eng.*, vol. 37, pp. 1193–1202, Apr. 1998.

[13] I. Baumann, R. Brinkmann, M. Dinand, W. Sohler, and S. Westenhöfer, "Ti : Er : $LiNbO_3$ waveguide laser of optimized efficiency," *IEEE Quantum Electron.*, vol. 32, pp. 1695–1706, Sep. 1996.